Mössbauer Effect Reference and Data Journal 3(8), 217-22 (1980)

COMPARISON OF TRANSMISSION AND SCATTERING METHODS USED IN MOSSBAUER SPECTROSCOPY

J. J. Bara and B. F. Bogacz

Institute of Physics, Jagiellonian University
Reymonta 4, 30-059 Cracow, Poland

The results of the comparison of line quality parameters, magnitudes of the Mössbauer effect and line widths of the absorption and the scattering spectra are presented.

I. INTRODUCTION

Although the transmission method is still most frequently used in Mössbauer spectroscopy (1, 2), continually increasing interest in scattering experiments has been lately observed (3). The scattering method is usually applied to special investigations such as high energy Mössbauer transitions, interference between the Rayleigh and nuclear resonance scatterings, bulk sample analysis and surface effects. It is in principle particularly suitable (4,5) for utilization in scientific investigations of the unique properties of Mössbauer spectroscopy such as high energy resolution and short observation time as well as the large value of the nuclear resonance cross section. Moreoever, as will be shown later, the scattering method may predominate the transmission method even in some conventional experiments.

It is the purpose of this paper to present the results of comparison of the transmission and the scattering methods.

II. COMPARISON OF ABSORPTION AND SCATTERING LINES

Let us consider the absorption and the scattering lines measured in the geometry of Fig. 1. A single line source is moved with a constant acceleration parallel to a beam direction. The gamma rays that pass through the sample under investigation and those scattered by it are independently detected and their intensities are simultaneously stored in the memory of a multichannel analyzer as functions of the source velocity. In this way Mössbauer absorption and scattering spectra are measured. Their corresponding parameters are the subjects of comparison.

The total number of gamma quanta that pass per second through the investigated sample at a given source velocity and then are registered in detector No. 1 is easy to calculate and is given by Eq. (1).

$$N(S) = \frac{f_a I_a}{\pi} d\omega_1 \exp(-\mu t \csc\beta_1) \int_{-\infty}^{\infty} \frac{\exp\left[-\frac{\mu_r t \csc\beta 1}{(y-S_1)^2+1}\right]}{(y-S)^2+1} dy + (1-f_a) I_a d\omega_1 \exp(-\mu t \csc\beta_1) \quad (1)$$

where y is the energy of a gamma quantum, S is the Doppler energy shift of the source, and S_1 is the isomer shift of the sample under investigation; all of the above are expressed in $\Gamma/2$ units. y and S_1 are given with respect to the mean value of the energy of Mössbauer gamma rays whose intensity and recoilless fraction are denoted by I_a and f_a, respectively. t is the thickness of the sample, while μ and μ_r are its electronic and nuclear resonance absorption coefficients, respectively. The angles β_1 and $d\omega_1$ are described in Fig. 1.

The total number of gamma quanta scattered per second, at a given source velocity toward the detector No. 2 is composed of five contributions and is given by Eq. (2).

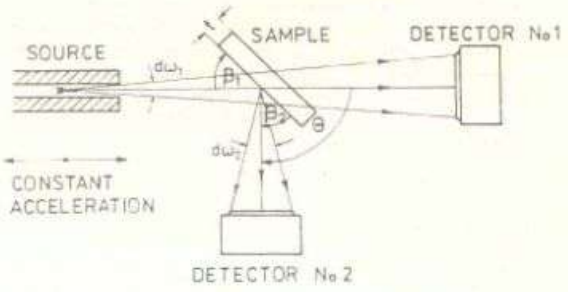

Fig. 1. Geometry used for the comparison of absorption and scattering spectra.

$$N(S) = N_{rr}(S) + N_{rn}(S) + N_{Rr}(S) + N_{R+C}(S) + N_{R+C} \qquad (2)$$

where

$$N_{rr}(S) = \frac{f_o (1-f_1) f_o \mu_r W_\gamma(\theta) \csc\beta_1 \, d\omega_1 \, d\omega_2}{\pi (1+\alpha) \mu (\csc\beta_1 + \csc\beta_2)} \int_{-\infty}^{\infty} Z_{\varkappa_r}(y,S)\, dy,$$

$$N_{rn}(S) = \frac{f_o (1-f_1) f_o \mu_r W_\gamma(\theta) \csc\beta_1 \, d\omega_1 \, d\omega_2}{\pi (1+\alpha) \mu (\csc\beta_1 + \csc\beta_2)} \int_{-\infty}^{\infty} Z_{\varkappa_n}(y,S)\, dy,$$

$$N_{Rr}(S) = \frac{f_o f_R(\theta) f_o \mu_R(\theta) \csc\beta_1 \, d\omega_1 \, d\omega_2}{\pi \mu (\csc\beta_1 + \csc\beta_2)} \int_{-\infty}^{\infty} [(y-S_1)^2 + 1] Z_{\varkappa_r}(y,S)\, dy,$$

$$N_{R+C}(S) = \frac{f_o f_o \{[1-f_R(\theta)]\mu_R(\theta) + \mu_C(\theta)\} \csc\beta_1 \, d\omega_1 \, d\omega_2}{\pi \mu (\csc\beta_1 + \csc\beta_2)} \int_{-\infty}^{\infty} [(y-S_1)^2 + 1] Z_{\varkappa_n}(y,S)\, dy,$$

$$N_{R+C} = \frac{(1-f_o) f_o [\mu_R(\theta) + \mu_C(\theta)] \csc\beta_1 \, d\omega_1 \, d\omega_2}{\mu (\csc\beta_1 + \csc\beta_2)} [1 - \exp(-T)],$$

while

$$Z_{\varkappa}(y,S) = \frac{1 - \exp\left[-T \dfrac{(y-S_1)^2 + \varkappa^2}{(y-S_1)^2 + 1}\right]}{[(y-S)^2+1][(y-S_1)^2 + \varkappa^2]},$$

$\varkappa_r^2 = 1 + \mu_r/\mu$, $\varkappa_n^2 = 1 + \mu_r \csc\beta_1/\mu(\csc\beta_1 + \csc\beta_2)$, and $T = \mu t (\csc\beta_1 + \csc\beta_2)$. The recoilless-recoilless $N_{rr}(S)$, recoilless-non-recoilless $N_{rn}(S)$ nuclear resonance, recoilless Rayleigh $N_{Rr}(S)$ and non-recoilless Rayleigh plus non-elastic Compton $N_{R+C}(S)$ contributions originating from recoil-free gamma rays, as well as the Rayleigh plus Compton contribution N_{R+C} orginating from non-recoillessly emitted gamma rays, are included in expression (2). θ is the scattering angle, $W_\gamma(\theta)$ is the angular distribution function for the resonantly scattered gamma rays, while α is the total internal conversion coefficient for a Mössbauer transition. The sample under investigation is characterized by its Rayleigh $\mu_R(\theta)$ and Compton $\mu_C(\theta)$ attenuation coefficients and its recoilless fractions f_1 and $f_R(\theta)$ for the nuclear resonance and Rayleigh scattering processes, respectively. The angles β_2 and $d\omega_2$ are described in Fig. 1.

From Eqs. (1) and (2) can be calculated the line amplitudes $N(\infty) - N(S_1)$, the magnitudes of the Mössbauer effect $\varepsilon(S_1) = [N(\infty) - N(S_1)]/N(\infty)$ and the line widths of the absorption and scattering lines. The experimental errors of these parameters depend on the quality of the measured spectrum. A Mössbauer spectrum is thought to be of high quality when the experimental points closely follow the theoretical line. Let us introduce the line quality parameter

$$Q = [N(\infty) - N(S_1)] / [\sqrt{N(\infty)} + \sqrt{N(S_1)}] \qquad (3)$$

which is determined by the ratio of the line amplitude to its statistical error. The line quality parameter increases with an increase in time interval τ of the storing Mössbauer line as the square root of τ. The line quality parameter is particularly suitable for comparison of Mössbauer absorption and scattering line intensities.

III. THE RESULTS

It is worthwhile to compare the line quality parameters, the magnitudes of Mössbauer effect and the line widths of Mössbauer absorption and scattering spectra measured in the geometry of Fig. 1. Eqs. (1) and (2) were used in the numerical calculation of these parameters. The 14.4 keV gamma rays of ^{57}Fe emitted with 0.05 steradian of a solid angle towards detector No. 1 and those scattered within 1.0 steradian towards detector No. 2 were considered. The calculations were performed for the first Zeeman line of the metallic iron foil of various thicknesses, various resonant isotope abundances and various hypothetical electronic absorption coefficients. The results obtained for the electronic absorption coefficient equal to 528 cm^{-1} correspond best to those of a real metallic iron foil.

The line quality parameters of absorption and scattering spectra and their ratios calculated for the non-enriched metallic iron foils of various thicknesses are shown in Fig. 2. Only for very thin and very thick samples the scattering method gives better results ($Q_A < Q_S$) than the transmission method as far as the intensity scale of the Mössbauer spectra is concerned. The ratios of line quality parameters calculated for samples of various parameters are shown in Fig. 3. The sample thickness intervals for which the transmission method gives better results ($Q_A > Q_S$) than the scattering one decrease with the increase in resonant isotope abundances and with the increase in the value of the electronic absorption coefficient.

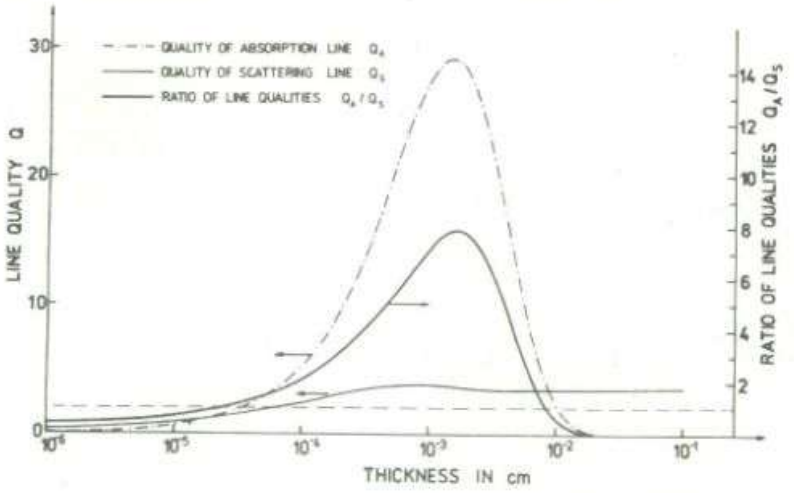

Fig. 2. The line quality parameters and their ratios calculated for the non-enriched metallic iron foils of various thicknesses.

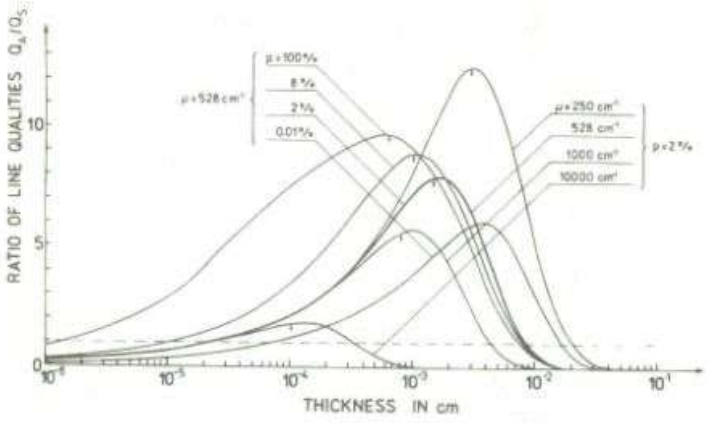

Fig. 3. The ratios of line quality parameters calculated for samples of various electronic absorption coefficients μ, resonant isotope abundances p and thicknesses. For samples of thicknesses larger than those marked by arrows, the scattering lines are narrower in comparison to the corresponding absorption lines.

The application of the scattering method always gives much higher values for the magnitude of the Mössbauer effect as compared with those obtained by the transmission method (Fig. 4). This is due to the filtrational properties of the nuclear resonance scattering process (4,5).

The line width of the absorption line does not depend on the value of the electronic absorption coefficient, whereas that of the scattering line does. This is illustrated in Fig. 5. In some cases the scattering line is narrower than the absorption one. The ratios of absorption and scattering line widths calculated for samples of various parameters are shown in Fig. 6. For thin samples, especially those of small values of electronic absorption coefficients, the absorption lines are narrower than the scattering ones ($\Gamma_t/\Gamma_s < 1$). For samples with large thicknesses the situation is reversed; the scattering lines are narrower in comparison to those of the corresponding absorption lines.

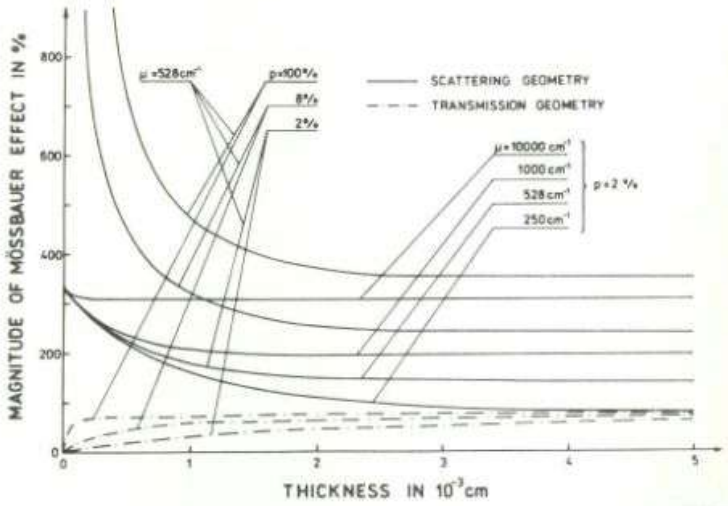

Fig. 4. The magnitudes of the Mössbauer effect of the absorption and scattering lines calculated for metallic iron foils of various thicknesses, resonant isotope abundances p and hypothetical electronic absorption coefficients μ.

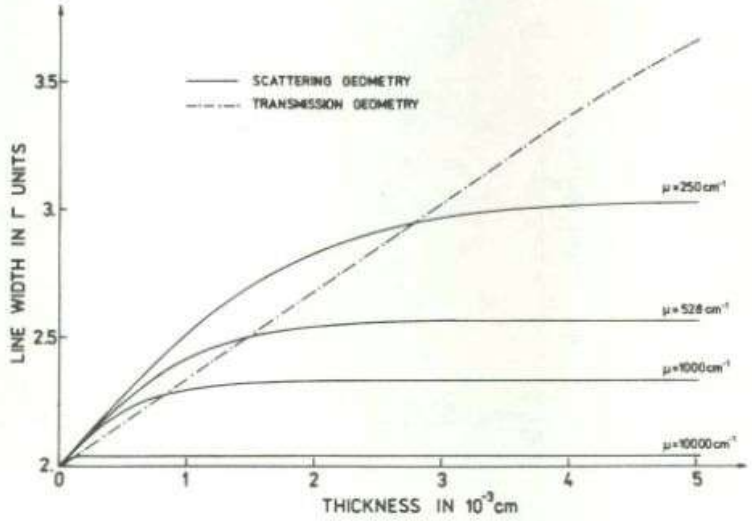

Fig. 5. The widths of absorption and scattering lines calculated for samples of various thicknesses and electronic absorption coefficients μ.

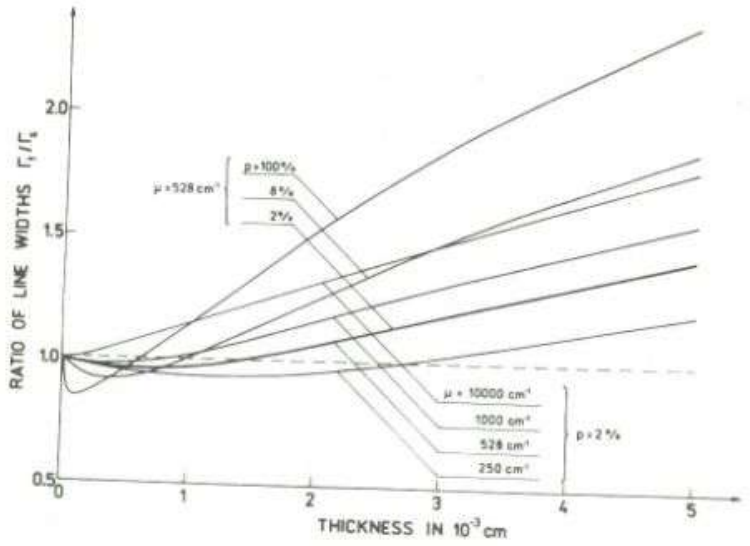

Fig. 6. The ratios of absorption Γ_1 and scattering Γ_s line widths calculated for samples of various thicknesses, electronic absorption coefficients μ and resonant isotope abundances p.

The line quality parameters and the line widths derived from the absorption and scattering spectra measured in the geometry of Fig. 1 for $2.3 \cdot 10^{-4}$, $1.6 \cdot 10^{-3}$, $2.0 \cdot 10^{-3}$, $3.5 \cdot 10^{-3}$ and $5.5 \cdot 10^{-3}$ cm thick metallic iron foils enriched to 95.15% by ^{57}Fe are shown in Figs. 7 and 8, respectively. The experimental data qualitatively confirm the theoretical results.

The ratios of line quality parameters were determined also for non-enriched hematite samples of various thicknesses. The uniform layers of hematite were obtained by sedimentation of a very fine polycrystalline powder in alcohol. The experimental results are in good agreement (Fig. 9) with those calculated for hematite Debye-Waller factor of 0.46 and electronic absorption coefficient of 225 cm^{-1} (6).

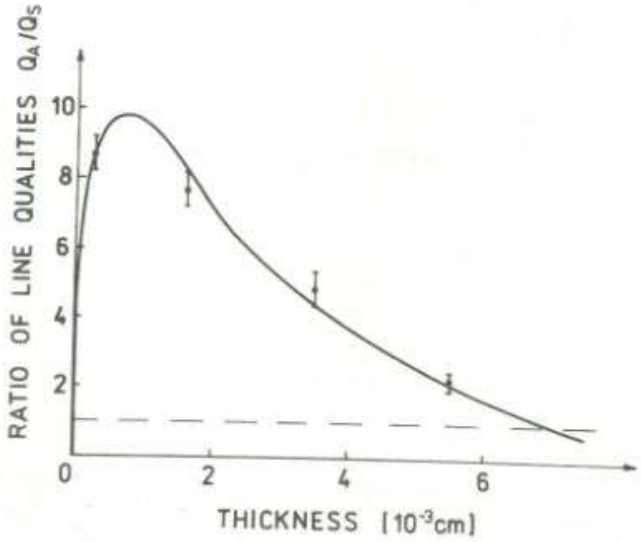

Fig. 7. The ratios of the line quality parameters of the first Zeeman lines of the absorption and scattering spectra measured for 95.15% enriched metallic iron foils of various thicknesses. The solid lines for absorption and scattering spectra were calculated from Eqs. 1 and 2, respectively.

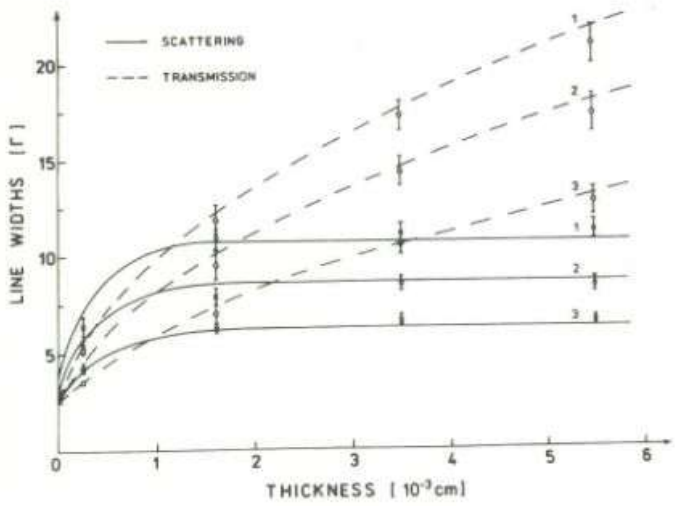

Fig. 8. The widths of Zeeman lines of the absorption and scattering spectra measured for 95.15% enriched metallic iron foils of various thicknesses. The dashed lines for absorption spectra were calculated from Eqs. 1 and 2, respectively.

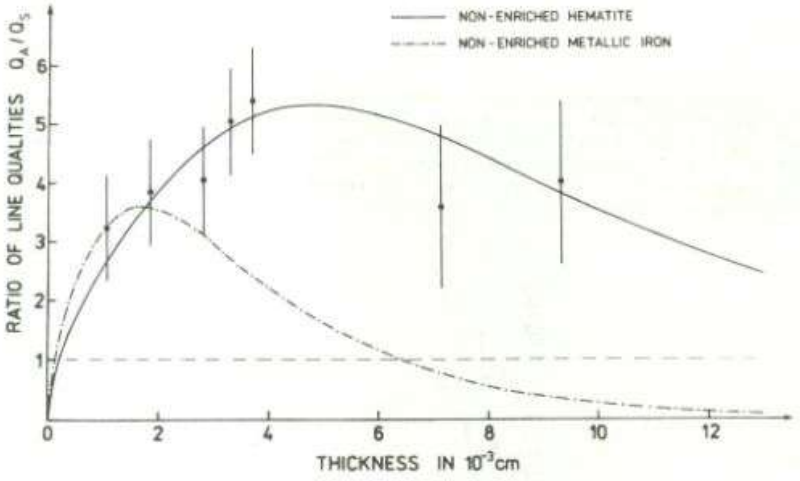

Fig. 9. The ratios of line quality parameters of the first Zeeman lines of absorption and scattering spectra measured for non-enriched hematite samples of various thicknesses. The results of Q_A/Q_S calculated for the first Zeeman line of non-enriched metallic iron foil are shown for comparison.

REFERENCES

1. A.H. Muir, Jr., K.J. Ando, and H.M. Coogan, Mössbauer Effect Data Index, 1958-1965 (Interscience, New York, 1966). J.G. Stevens, V.E. Stevens, P.T. Deason, Jr., A.H. Muir, Jr., H.M. Coogan, and R.W. Grant, Mössbauer Effect Data Index, 1966-1968 (IFI/Plenum, New York, 1975). J.G. Stevens and V.E. Stevens, Mössbauer Effect Data Index, 1969-1974 (IFI/Plenum, New York).
2. Schnellinformation Mössbauer Spektroskopie, 1972-1977 (Akademie der Wissenschaften der DDR, Berlin).
3. F.E. Wagner, J. Phys. (Colloq.) 37, C6-673 (1976).
4. J.J. Bara, INP Report No. 1011/PL, 1978.
5. J.J. Bara, Hyperfine Interactions, Proceedings (XVII Winter School, Bielsko-Biata, 1979), p. 226.
6. J.J. Bara, B.F. Bogacz, Phys. Status Solidi A 44, K107 (1977).